

CONTRIBUTION OF REMOTE SENSING IN THE STUDY OF THE EVOLUTION OF A SHORELINE: APPLICATION TO THE CAMEROONIAN LITTORAL COAST

J. Fotsing^{a,*}, E. Tonyé^a, N. T. Tankam^a, T. F. N. Kanaa^a, J. P. Rudant^b

^a NASE, National Advanced School of Engineering, Yaoundé, Cameroon - (jfotsing, ntalla)@gmail.com, tonyee@hotmail.com, t_kanaa@yahoo.fr

^b Institut Francilien des Géosciences, Laboratoire des Géomatériaux, 5 Boulevard Descartes, Champs-Sur-Marne, Université de Marne-La-Vallée, France - rudant@univ-mlv.fr

KEY WORDS: Remote sensing, coastal waterways, shorelines, littoral coast, Cameroon

ABSTRACT:

Cameroon's coast is a great asset for tourism and the economic recovery of Cameroon. There is a recent population surge towards the coast of Cameroon, which calls for attention to the balance between urban areas and natural areas. It is therefore imperative to promote business development and jobs related to the coasts, coastal waterways and shorelines of lakes on the one hand and meet the environmental challenge presented by the steady erosion of the sandy and rocky shoreline which is risky to the population and surroundings. The coastal area is a particularly fragile area coveted by fishermen, traders, industries (oil) and tourism professionals. It is therefore necessary to limit the risks incurred by these populations increasingly attracted to the coastal shores.

The aim of this project is to study the behaviour of the littoral coast with time. Considering global warming which is a international problem; the question is whether this situation has no impact on Cameroon's littoral coast. It is a question of whether, over time, the coast remains static or the ocean claims or frees up ground space. In the case of a dynamic shoreline, it is a question of whether this motion is uniform or random in order to estimate the rate at which the ocean claims or frees living area.

RÉSUMÉ:

Le littoral camerounais est un formidable atout pour la valorisation touristique et économique du Cameroun. On observe une poussée démographique récente vers les côtes camerounaises qui incite à renforcer l'attention au respect des équilibres entre les zones urbanisées et les zones naturelles. Il apparaît dès lors impératif de promouvoir le développement des activités et des emplois liés au littoral, aux côtes fluviales et aux rivages des grands lacs d'une part et de relever le défi écologique, avec l'érosion régulière du littoral sableux et rocheux qui présente des risques pour les populations et pour les territoires. Le littoral constitue un espace particulièrement fragile et convoité par les pêcheurs, les commerçants, les industriels (pétrole) et les professionnels du tourisme. Il convient dès lors de limiter les risques encourus par ces populations de plus en plus attirées vers les côtes littorales.

Le but de ce projet consiste à étudier le comportement de la côte littorale avec le temps. Compte tenu du réchauffement de la planète qui est une préoccupation mondiale, la question est de savoir si cette situation n'a pas d'impact sur la côte littorale Camerounaise. Il est question de voir si avec le temps la côte reste statique ou alors si l'océan gagne ou libère de l'espace terrestre. En cas de dynamisme de la ligne de rivage, il est question de voir si ce mouvement est uniforme ou aléatoire afin d'estimer la vitesse de gain ou de recul de l'océan de la surface habitable.

1. INTRODUCTION

Cameroon's coast is a great asset for tourism and the economic recovery of Cameroon. There is a recent population surge towards the coast of Cameroon, which calls for attention to the balance between urban areas and natural areas. The coast is a particularly sensitive area (the sea is not always predictable) and coveted by fishermen, traders, industries (oil) and tourism professionals. It is therefore necessary to limit the risks incurred by these populations increasingly attracted to the coastal shores. Capital to this struggle is the study of the behaviour of the littoral coast with time. The preferred method is the use of remote sensing images. The processing of these images is done by texture analysis.

The textural analysis was, primarily, the extraction of structural parameters and statistics describing the distribution of intensity variations in the image. Many techniques of texture analysis

exist (Haralick, 1986; Reed and Du Buf, 1993; Marceau et al., 1990; Maillard, 2001) and can be classified into two broad categories. On the one hand, it distinguishes statistical methods based on the calculation of statistics inherent in the texture (Haralick, 1986; Talla 2008), and on the other, methods based on structural description of texture primitives and their arrangement (Kourgly, 1997). The proposed method here is a structural approach using an experimental variogram and two empirical variogram models to extract texture parameters. With these two models (we have four parameters) in which each pixel is characterized by a feature vector whose components, known as Range, Sill, Slope and Fractal Dimension, are constants deduced from the fitted models. The parameters deduced from the experimental variogram are included in a classification process.

* Corresponding author

The aim of this paper is to study the dynamics of Cameroon's coast with time. Being limited by the number of images, we present, here, a technique for extracting Cameroon's littoral coastline from a satellite radar image of ERS-1. Indeed, a sufficient number of satellite radar images would provide the means for studying these dynamics by extracting the coastline, from each image and through the merging of different features extracted. Merging thus would provide for observation of the evolution of Cameroon's coastline with time. To extract the coastline, we use the structural methods in a supervised classification approach. The particularity of this approach lies in the fact that each pixel is fully characterized by its texture vector. Indeed, the texture vector gives better information of the pixel because it takes into account the neighboring pixel considered. The approach to classification of radar images by texture vector is quite unique in that it allows a better characterization of each pixel of the image. In effect, each pixel is assigned a window of the image centred on the pixel. This pixel is then characterized by the properties of the window. In the following, we will present the notion of variogram and texture parameters, followed by the criteria of the image window and the training zones. Once the characterization of the various training zones is done and the classification algorithm is presented. Finally, we present some experimental results.

2. METHODOLOGY

2.1 Variogram and numerical image

2.1.1 Variogram formulation: Traditionally, variograms have been used for modelling spatial variability rather than the covariance although kriging systems are more easily solved with covariance matrices. In this study, we analyzed the spatial distribution property of each image through variogram.

The variogram must be checked for changes in values based on different directional orientation, known as anisotropy (Kourgly and Belhadj-Aissa, 2003); however, anisotropy is rarely significant in imagery variograms.

To estimate a variogram, we consider two numerical values of image, $L(x, y)$ and $L(x+h, y+v)$, established in two pixels distant by a vector (h, v) . We characterize the variability between the two intensities by variogram function $2\gamma(h, v)$ defined as variable expectancy.

$$2\gamma(h, v) = \frac{1}{(N-h) \times (M-v)} \sum_{i=1}^{N-h} \sum_{j=1}^{M-v} [L(x_i, y_j) - L(x_i+h, y_j+v)]^2 \quad (1)$$

Then, the estimator $2\gamma(h, v)$ is equal to the mathematical average of the gap quadratics between two intensities $[Z(x_i, y_j), Z(x_i+h, y_j+v)]$:

$$2\gamma(h, v) = \frac{1}{(N-h) \times (M-v)} \sum_{i=1}^{N-h} \sum_{j=1}^{M-v} [L(x_i, y_j) - L(x_i+h, y_j+v)]^2 \quad (2)$$

where $(N-h) \times (M-v)$ is the number of the experimental pairs. For one numerical image $I(i, j)$ of size $N \times M$, we can estimate the duplex variogram according to different directions (angles).

For the four directions, we obtain the following formulations:

❖ For the horizontal direction (angle = 0°)

$$2\gamma(h) = \frac{1}{N \times (M-h)} \sum_{i=1}^N \sum_{j=1}^{M-h} [I(i, j) - I(i, j+h)]^2 \quad (3)$$

where $I(i, j)$ is the associated gray level of pixel in position (i, j) , h is the lag, N is a number of lines and M is a number of columns.

❖ For the vertical direction (angle = 90°)

$$2\gamma(h) = \frac{1}{(N-h) \times M} \sum_{i=1}^{N-h} \sum_{j=1}^M [I(i, j) - I(i+h, j)]^2 \quad (4)$$

❖ For the diagonal 1 direction (angle=45°)

$$2\gamma(h) = \frac{1}{(N-h) \times (M-h)} \sum_{i=1}^{N-h} \sum_{j=1}^{M-h} [I(i, j) - I(i+h, j+h)]^2 \quad (5)$$

❖ For the diagonal 2 direction (angle=135°)

$$2\gamma(h) = \frac{1}{(N-h) \times (M-h)} \sum_{i=1}^{N-h} \sum_{j=1}^{M-h} [I(i, j) - I(i-h, j+h)]^2 \quad (6)$$

2.1.2 Modelling functions: Once a variogram is obtained, the spatial covariance structure can be quantified by choosing a variogram model. Usually a model is chosen to minimize a fitting criterion such as the sum of least square. The equations for these models are:

Exponential model

$$\gamma(h) = C \left(1 - e^{-h/H_p} \right) \quad (7)$$

where C is a constant that denotes the highest values of γ (the "Sill"), and H_p denotes the distance where the variogram effectively becomes level (the "Range").

Fractal model

$$\gamma(h) = Kh^\alpha \quad (8)$$

where K is a constant that denotes continuity crossing of γ (the "Slope") and α denotes the exponent of variability.

For the phenomena which in a scale h present a self-similarity, we know that the variogram verifies the equation given below.

$$\gamma(h) = Kh^{2(3-D)} \quad (9)$$

where D is a fractal dimension of the phenomenon (Mandelbrot, 1982). Hence, for the models whose variograms are defined by equation (8), we can define the fractal dimension of the texture image by the equation given below.

$$D = 3 - \frac{\alpha}{2} \quad (10)$$

Note that, a variogram is generally also characterized by a parameter known as nugget effect. The nugget effect is the discontinuity at the origin. In our case, there was no nugget effect. In fact, relations (3), (4), (5) and (6) show that $\gamma(0) = 0$.

2.2 Contour detection

2.2.1 Principle of determination: Usually, the determination of the contours is based on operators of the mathematical

morphology (Akono et al., 2006). The operators of the mathematical morphology apply to binary images, but it can also be applied on gray level image (Serra, 1982). In this study, we use feature vector deduced on the experimental variogram to extract the contour. To extract the contour, we transform firstly the gray level image in binary image. To have the binary image, we extract a homogeneous training zone of size $T_x \times T_y$ from the image. The training zone is then modeled by a feature vector where the components (Slope, Range, Sill and Fractal Dimension) are calculated by using the interpolation of experimental variogram and the two theoretical models. The method of calculation of texture parameters is presented in Fotsing et al. (2009). We apply secondly the algorithm of classification. The classification consists in the extraction of principal layer information previously characterized by texture known as training zone. On the line of separation of the two classes, we take a series of training zones that we characterize by the same method. The feature vector of the shoreline is equal to the average of the different results obtained by each training site. We apply again the algorithm of classification. The result obtained in this final phase will then relate the contour sought. The optimal window sizes that could achieve the highest classification accuracy were investigated. Optimal window sizes are selected based on better characterization of spatial patterns land-use categories with less boundary effect. The boundary effect refers to the situation that assigning class for a pixel which is close to the boundary of two or more neighboring classes is confused within a window (Gong et al., 2003). The dilemma was that the pixel window size should not be too small or too big. When the window was too small to contain enough information class pixels to analyze their spatial relationship, the derived semi-variance would not represent the texture well as a whole. When the window was too large, the straddled two neighboring classes and the derived semi-variance was a mixture of class textures. In other words, too small window sizes caused high within-class variation and too large windows caused high between-class confusion. Both extreme window sizes cast difficulty on the classification. Optimal window sizes were usually decided empirically (e.g., Gong et al., 2003, Gong and Howarth 1992), so were optimal lags (e.g., Gong and Howarth 1992). In this study, we investigated the optimal window sizes through accuracy of classification (Kappa coefficient).

2.2.2 Algorithm for extraction layer information: In the classification phase, the adopted approach consists in the extraction of a single layer at a time. A fusion is then made to the various extracted classes and the global classification with the various classes of soil occupation is obtained. To extract a given class X , the following operations are carried out after the order.

1. Extraction of an image window W entirely enclosed in the class X ;
2. Select the direction of calculation of texture parameters;
3. Calculation and representation of the experimental variogram and fitting it with the two functions model by using the least square criterion;
4. Deduction of texture parameters. In this step, the fitted model is quantified through its coefficients such as Range and Sill (deduced on the exponential model (7)) and Slope and Fractal Dimension (deduced on the fractal model (8));

5. Construction of a feature vector V_{CC} with the various parameters previously extracted;
6. For each pixel of the image, do the following instructions:
 - a) Extraction of an image window F , with size W and centered on the pixel i ;
 - b) Do the steps 2 to 4 described above;
 - c) Construction of a feature vector V_i with the various parameters previously extracted;
 - d) Evaluation of the distance between V_{CC} and V_i by the formula given below;

$$d_i = \sqrt{\sum_{k=1}^4 (V_{CC}(k) - V_i(k))^2} \quad (11)$$

$$T = \frac{d_i}{d_{\max}} \times 100$$

- e) If the threshold d_{\max} is less than a certain value (less than 5% in general), then the pixel i belongs to the class X . If not, the pixel i does not belong to the class X .

d_{\max} is the maximum distance between the feature vectors of two image windows with the same size as W on the image.

3. EXPERIMENTATION

3.1 Experimental zone and data used

This approach has been experimented on an ERS-1 SAR image (Figure 1a) of the Atlantic coast of Cameroon, registered in band C (5.66 cm of wave length) and in VV (vertical-transmit, vertical-receive) polarization with a resolution of 12.5m. Using topographical and lithographical charts at a scale 1:200 000, we identified two main classes of soil occupation on the image of the site of study. The first class, identified by the training zone A (Figure 1b) represents the sea zone, the second class identified by the training zone B (Figure 1c) represents the separating line between ocean and soil occupation. In this study, the training zone B is extracted after extraction the ocean information class (Figure 4b). The ERS-1 SAR image was taken on October, 1994. This data was received in the Libreville's (Gabon) station of the European Space Agency (ESA).

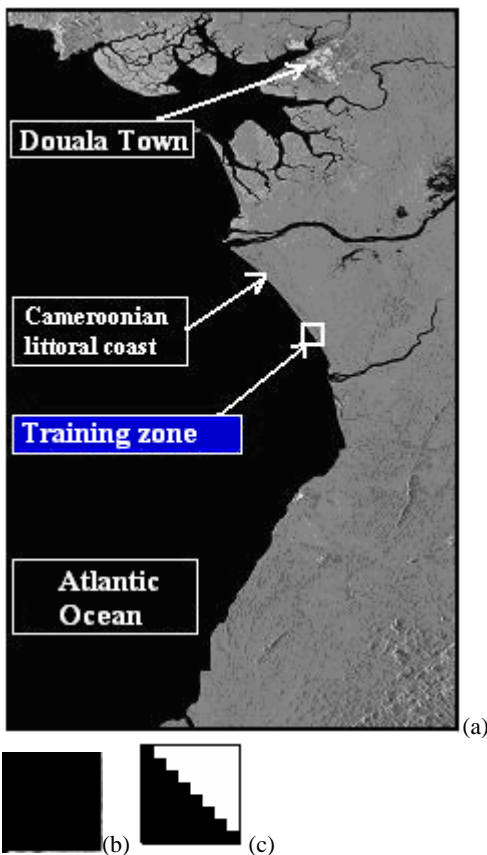


Figure 1. (a) Global view of the site study; (b) Zone A; (c) Zone B

3.2 Characterization of training site

Figures 2 and 3 present the example of characterization of structural information deduced from a textural pattern of the two training zones (Zone A and Zone B). To practice, we show on the graphs (Figures 2 and 3) the interpolation of the experimental variogram (green color) with empirical variogram (yellow color). Figure 2a helps to deduce the parameters (Sill) $C_A = 347.44$ and (Range) $H_{pA} = 2$ given by the exponential model (7) and figure 2b the two other parameters (Slope) $K_A = 268$ and (Fractal Dimension) $DF_A = 2.87$ given by the fractal model (8). Figure 3a gives by using exponential model the following parameters: (Sill) $C_B = 2757.66$ and (Range) $H_{pB} = 6$ and the figure 3b with fractal model (Slope) $K_B = 1210.78$ and (Fractal Dimension) $DF_B = 2.81$.

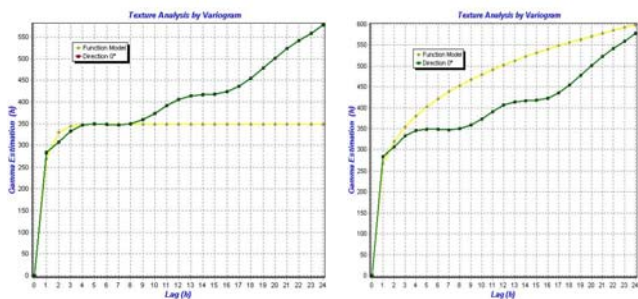
Numerically, the various training zones A and B are respectively characterized by the following feature vectors: $V_A = (2; 347.44; 268; 2.87)$, $V_B = (6; 2757.66; 1210.78; 2.81)$.

3.3 Experimental result and discursion

Figures 2, 3 and 4 show the representation of the different results obtained in this study. These results are obtained through the software created as part of our research work. This software, called VOIR+ (Vision par Ordinateur des Images Radar Plus) was developed with the environment of Borland C++ Builder 6. Figure 4b shows the classification results obtained by applying the algorithm proposed with optimized windows size 9×9 in the direction East-West. This figure 4b highlights the extraction of the information layer on the sea (black color). Figure 4c shows the extraction of information layer on the coastline always obtained by applying the classification algorithm proposed. The windows size 7×7 was used to extract the coastline in the direction South-West / North-East.

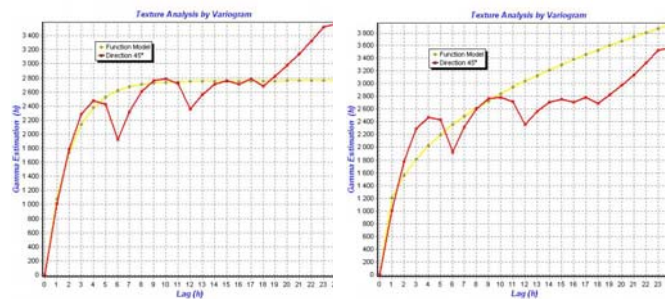
Figure 4a shows the SAR image of ERS-1 study site. Figure 4b shows the ocean (black color) of the coastal littoral Cameroon extracted from this image. Figure 4c shows the shoreline of the Cameroon coast extracted from this image. Figure 4d shows the fusion of the shoreline with the original image (Figure 4a). The roughnesses of the northern sector are extracted. In addition, the river located south of Douala was also noted. By merging, the figures 4a and 4c reveals that, the major axes of the river system have been identified and there is a perfect match between the coastline and sample the original image (Figure 4d).

From a set of multi-temporal images, it would be possible to study the dynamics of the shoreline of the coast and coastal Cameroon able to estimate the length of the coastline. Indeed, it would be enough for each image, apply the same methodology to extract shoreline. Once the various shorelines extracted from a merger in the manner of image (Figure 4d) would see the evolution of this coast. If all lines are confused, then we conclude that the coast is static. If the lines are progressively West-East direction, we say that the sea reaches the shore in time. If it is in an East-West, we conclude that the sea recedes with time. In one or the other case, by calculating the number of pixels separating the first line of the last and knowing the pixel resolution, we could estimate the distance gained or lost by the sea in 10 years. And if at times there is a change of direction, we conclude that the shoreline has a random behaviour. However, we can assess the general trend for the last 10 years. In this work, do not have enough images of the study site in order to study the dynamics of the coastal side. We limit ourselves just to extract this shoreline.



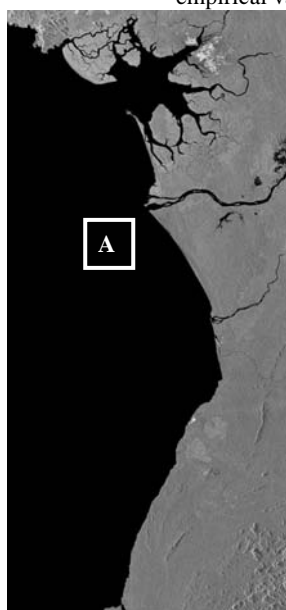
(a) Interpolation of experimental variogram (green) with exponential model (yellow)
 (b) Interpolation of experimental variogram (green) with power model (yellow)

Figure 2. Characterization of texture using experimental and empirical variogram (Zone A)



(a) Interpolation of experimental variogram (red) with exponential model (yellow)
 (b) Interpolation of experimental variogram (red) with power model (yellow)

Figure 3. Characterization of texture using experimental and empirical variogram (Zone B)



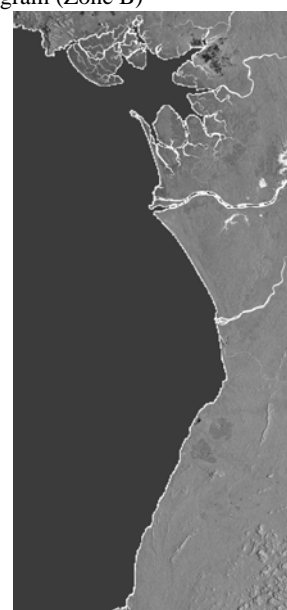
(a) Original image



(b) Extraction of the class Sea (Black color)



(c) Extraction of the coastline (Black color)



(d) Result of the fusion applied after extraction of the coastline

Figure 4. Result of classification using spatial covariance information

4. CONCLUSION

The processing of SAR images of ERS-1 for the extraction of Cameroon's littoral coastline relies on the concept of texture vector in a supervised classification. The relevant parameters of texture are selected on the basis of their ability to describe the experimental variogram. In this work, the directions East / West and South-West / North-East are used and the segmentation is performed using several training sites well known and representing the same theme (Earth / Sea separating line). This approach is promising in view of the results obtained. Monitoring and estimating the length of Cameroon's coastline and tracking phenomena of low flows and flood waters would be possible if many images of this same coastline on various dates were available to us.

ACKNOWLEDGEMENTS

This work was supported by the LETS laboratory of the National Advanced School of Engineering of the University of Yaoundé I. We are also grateful unto the European Spatial Agency (ESA) for the grant of SAR ERS-1 image used in this study.

REFERENCES

- Akono A., Talla T. N., Tonyé E., Nyoungui A. N., Dipanda A., 2006. High Order Textural Classification of two SAR ERS images on Mount Cameroon. *Geocarto International*, Vol. 21, N°3.
- Fotsing, J., Tonyé E., Talla Tankam N., and Rudant J.P, 2009. Modélisation de la texture par le biais de l'analyse variographique. *Proceedings of the IEEE, SETIT'09*, 22-26

march, Hammamet, Tunisia (5th International Conference Sciences of Electronic, Technologies of Information and Telecommunications), unpaginated CD-ROM.

Gong, P., and Howarth P.J., 1992. Frequency-bases contextual classification and gray-level vector reduction for land use identification. *Photogrammetric Engineering & Remote Sensing*. 58(4): pp. 423-437.

Gong,B.P., Spear R., and Seto E., 2003. Comparison of different gray level reduction schemes for a revised texture spectrum method for land use classification using Ikonos imagery. *Photogrammetric Engineering & Remote Sensing*. 69(5): pp. 529-536.

Haralick, R. M., 1986. *Statistical Image Texture Analysis*. Chapter 11 of Handbook of Pattern Recognition and Image Processing. Academic Press Edition, pp. 247-279.

Kourgli, A. et Belhadj-aissa, A., 1997. Approche structurale de génération d'images de texture. *International Journal of Remote Sensing*. N° 17, Vol. 18, pp. 3611-3627.

Kourgly A., Belhadj-Aissa A., 2003. Segmentation texturale des images urbaines par le biais de l'analyse variographique. *Téledétection*. Vol. 3, N° 2-3-4, pp. 337-348.

Maillard P. 2001. Developping methods of texture analysis in high resolution images of the Earth. *Anais X SBSR, Foz do Iguacu*, 21-26 abril 2001, INPE, pp. 1309-1319.

Mandelbrot B., 1982. *The Fractal Geometry of Nature*. San Francisco, W. H. Freeman.

Marceau, D.J., Howarth, P.J., Dubois, J-M. M. and Gratton, D.J., 1990. Evaluation of the Grey-Level Co-Occurrence Matrix Method for Land-Cover Classification Using SPOT Imagery. *IEEE Transactions on Geoscience and Remote Sensing*, Vol. 28, N° 4, pp. 513-518.

Reed, T. R. and Du Buf J. M. H., 1993. A Review of Recent Texture Segmentation and Feature Extraction Techniques. *CVGIP: Image Understanding* vol. 57, N° 3, pp. 359-372.

Serra, J., 1982. *Image analysis and mathematical morphology*. Academic Press, London, 628 p.

Talla T. N., Dipanda A., Tonyé E., 2008. Nouvelle approche d'évaluation des paramètres de texture d'ordre supérieur pour l'analyse automatique d'images numériques. *Revue santé/STIC de l'Université de Bourgogne*, N°3: pp. 102-105.